Effect of high-energy heavy ion irradiation on the crystallization kinetics of Co-based metallic glasses

ROHIT JAIN, DEEPIKA BHANDARI, N S SAXENA*, S K SHARMA[†] and A TRIPATHI[‡]

Department of Physics, University of Rajasthan, Jaipur 302 004, India
[†]Department of Physics, Malaviya Regional Engineering College, Jaipur 302 017, India
[‡]Nuclear Science Centre, Aruna Asaf Ali Marg, New Delhi 110 067, India

Abstract. Differential scanning calorimeter (DSC) is employed to study the crystallization kinetics of irradiated (at three different fluences with high-energy heavy ion; Ni^{11+} of 150 MeV) specimens of two Co-based metallic glasses. It is found that the crystallization process in both the glasses is completed in two phases. The DSC data have been analysed in terms of kinetic parameters viz. activation energy (E_c), Avrami exponent (n), dimensionality of growth (m), using two different theoretical models. The results obtained have been compared with that of virgin samples. The lower activation energy in case of second crystallization occurring at higher temperature indicates the easier nucleation of second phase. The abnormally high value of Avrami exponent in Co–Ni glass indicates very high nucleation rate during first crystallization.

Keywords. Crystallization kinetics; high-energy heavy ion irradiation; morphology.

1. Introduction

The ion-beam assisted techniques have made substantial contributions as a selective tool for understanding, fabricating and characterization of amorphous alloys (Appleton *et al* 1985; Rauhala *et al* 1998). The effect of low energy heavy ion irradiation (up to 500 keV) on the crystallization kinetics of metallic glasses have been reported by Köster and Herold (1981) and Zhou *et al* (1994). The crystallization temperature is found to decrease significantly due to heavy ion irradiation at low energy. However, not much attention has been paid to investigate the effect of high-energy irradiation (more than 500 keV) on the stability against the crystallization of metallic glass. An ion penetrates a solid and slows down (i) by direct transfer of energy to nuclei by elastic collisions and (ii) by electronic excitation and ionization of atoms by inelastic collision. The two processes are known as nuclear energy loss, S_n, and electronic energy loss, S_e, respectively. At high energies (i.e. fast ions), the predominant mechanism for energy loss is electronic. When the radiation passes through the matter, it causes damage, which depends on the type and the energy of the radiation and the properties of the medium. It is generally pictured that atomic displacements are primarily induced by elastic collisions and not by electronic excitation or ionization. However, slowing down of heavy ions in insulator targets is known to induce structural changes called latent tracks.

Now it has been established (Klaumunzer and Schumachar 1981; Mehta 1994) that electronic excitations can also provoke structural changes in materials. The understanding of the operative mechanisms, however, is quite incomplete. In view of this, an attempt has been made to investigate the effect of high-energy heavy-ion irradiation on the crystallization kinetics of two Co-based metallic glasses. For irradiation at different fluences, the Ni^{11+} ions of 150 MeV have been used. The crystallization kinetics is the most convenient method as the sequence of phase during crystallization process provides the direction to see any structural changes due to irradiation. The crystallization process has been investigated using differential scanning calorimeter (DSC) under non-isothermal condition. The experimental data are analysed using two theoretical models developed by Kissinger (1956) and Gao and Wang (1986) in terms of kinetic parameters viz. activation energy, Avrami exponent and dimensionality of growth. The kinetic parameters obtained have been compared with that of virgin glasses.

2. Experimental

The multi-component metallic glasses viz. $Co_{66}Si_{16}B_{12}Fe_4Mo_2$ and $Co_{66}Si_{15}B_{14}Fe_4Ni_1$ (referred to as Co–Mo and Co–Ni respectively hereafter) were cut in suitable size of 1×1 cm^2 for irradiation purpose. The specimens were cleaned ultrasonically and no thermal treatment was given to the samples prior to irradiation. The samples were stuck to the copper ladder for irradiation with the help of

---

*Author for correspondence

silver paint. The continuity of the samples was checked before putting the ladder in vacuum chamber. The samples were irradiated with Ni^{11+} ion beam of 150 MeV energy at three different fluences ranging from 10^{11} to 10^{13} ions/cm^2 at the Nuclear Science Centre, New Delhi. The projected range for 150 MeV Ni^{11+} ions was calculated using Trim program for both the glasses, indicating that probability of ion implantation is negligible. Only one irradiation geometry was used in this work, viz. the surface normal of the specimens was aligned parallel to the ion beam. The amorphous nature of all the irradiated and virgin samples was confirmed by X-ray diffraction.

DSC study was performed on Rigaku 8230 B attached with thermal analysis station (TAS) to see the effect of irradiation on the crystallization kinetics of glass under non-isothermal condition. The samples were scanned from room temperature to 975 K in dry nitrogen flowing at 30 ml/min atmosphere at different heating rates: 5, 7, 10, 15 and 20 K/min. The instrument was calibrated prior to measurement using high purity standards of indium and lead with well known melting points and latent heat. The calibration and measurements of glasses were carried out under identical conditions for better accuracy.

3. Results and discussion

Figures 1 and 2 show the DSC traces of irradiated Co–Mo and Co–Ni metallic glasses at three different fluences at a heating rate of 20 K/min. The DSC thermogram of virgin glasses at the same heating rate is also shown in the respective figures for comparison point of view. All the

thermograms (for virgin as well as irradiated samples) have well defined exothermic peaks indicating the occurrence of crystallization. However, in these glasses the crystallization is incomplete in a single stage. The Co–Mo glass exhibits two overlapping peaks of crystallization along with a small shoulder in the first peak at higher temperature side. This shoulder is clearly observed at relatively higher heating rates. The shoulder found on the higher temperature side of the main peak does not indicate the presence of any new phase, rather it is a manifestation of the delayed crystallization of the small portion of the glass that was adjacent to the wheel during spinning and hence experienced the most rapid cooling. As a result of the high quench rate, this part of the ribbon has much fewer (or no) quenched-in nuclei, and so crystallizes at relatively higher temperature. A similar type of shoulder has also been found in many other glasses e.g. $Fe_{80}B_{20}$ (Greer 1982), $Al_{75}Cu_{15}V_{10}$ (Holzer and Kelton 1991) and $Ni_{72}Mo_2Co_6B_{20}$ (Graydon *et al* 1995). It was reported that the shoulder found for $Fe_{80}B_{20}$ glass was due to delayed crystallization for the 10% of the ribbon nearest to the wheel, and, when crystallized, this portion showed the identical phases as were found in the bulk of the glass (Greer 1982). The delayed crystallization is ascribed to the necessity to first develop nuclei in the rapidly cooled zone. On the other hand, the Co–Ni glass has two peaks separated by wide temperature interval. In Co–Ni glass, the second peak is not very clearly distinguished in DSC trace as the first and second peaks differ too much in magnitude. Figure 3 is given as a representative curve for the second peak with the stretched heat flow axis at the heating rate of 20 K/min. The first peak in both the glasses indicate hcp Co-solid solution while the second
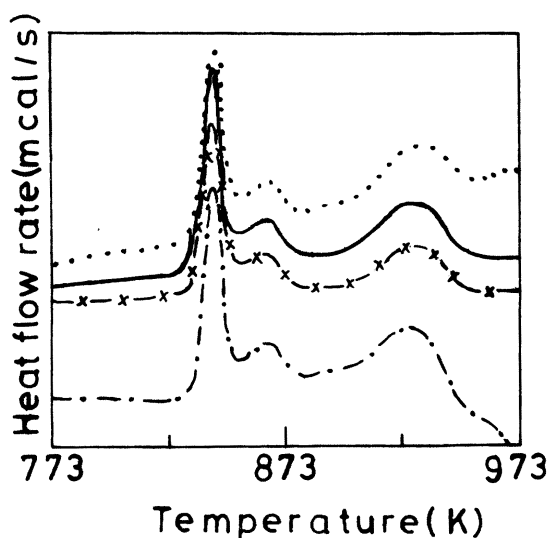

Figure 1. DSC thermograms of virgin and irradiated Co–Mo glass at the heating rate of 20 K/min (— Virgin; –×–×–×– irradiated at fluence 1×10^{11} ions/cm^2; –•–•–•– irradiated at fluence 1×10^{12} ions/cm^2; • • • irradiated at fluence 1×10^{13} ions/cm^2).
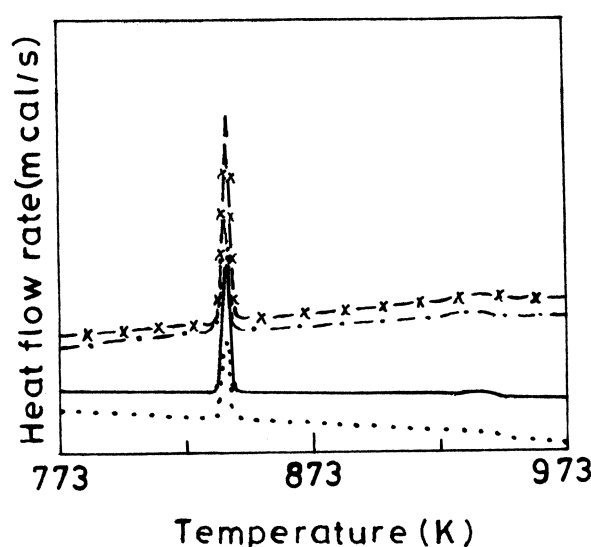
Figure 2. DSC thermograms of virgin and irradiated Co–Ni glass at the heating rate of 20 K/min (— Virgin; –×–×–×– irradiated at fluence 1×10^{11} ions/cm^2; –•–•–•– irradiated at fluence 1×10^{12} ions/cm^2; • • • irradiated at fluence 1×10^{13} ions/cm^2).
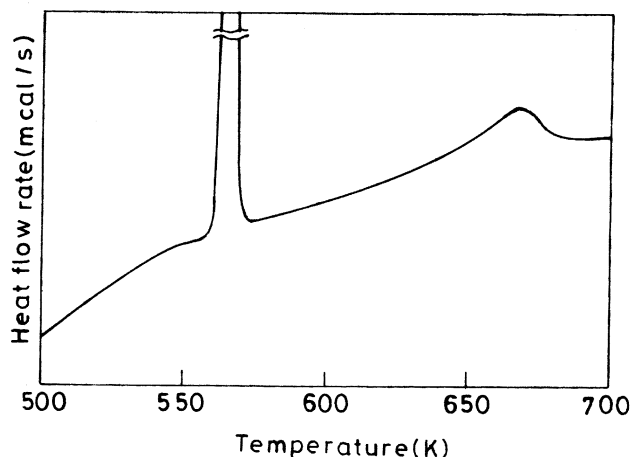
Figure 3. DSC trace of Co–Ni glass at the heating rate of 20 K/min as a representative curve for showing the difference in magnitude of the two peaks of crystallization.
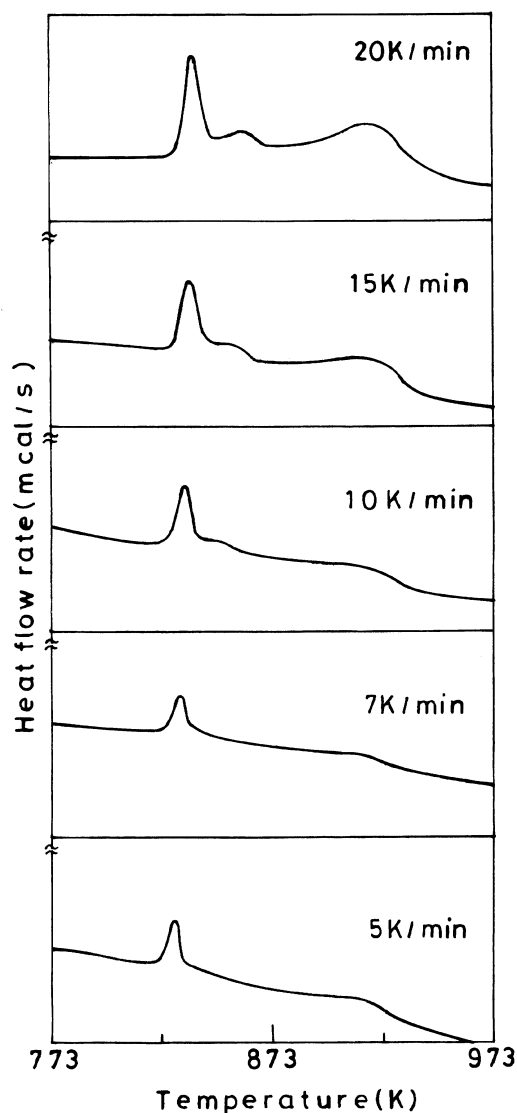
peak shows body centred tetragonal (b.c.t.) Co_3B phase (Wang and Meng 1983).

Further, it is clear from the figures that there is no substantial change in the crystallization temperatures (T_c) and peak crystallization temperatures (T_p) after the high-energy heavy ion irradiation at different fluences ranging from 10^{11} to 10^{13} ions/cm². Similar observations have also been noticed at other heating rates. The DSC thermograms of one irradiated specimen (fluence: 1×10^{13} ions/cm²) from each glass at all the heating rates employed here are shown in figures 4 and 5 as representative curves.

Figure 4. DSC thermograms of irradiated Co–Mo glass at the heating rate of 5 K/min, 7 K/min, 10 K/min, 15 K/min and 20 K/min (fluence: 1×10^{13} ions/cm²).

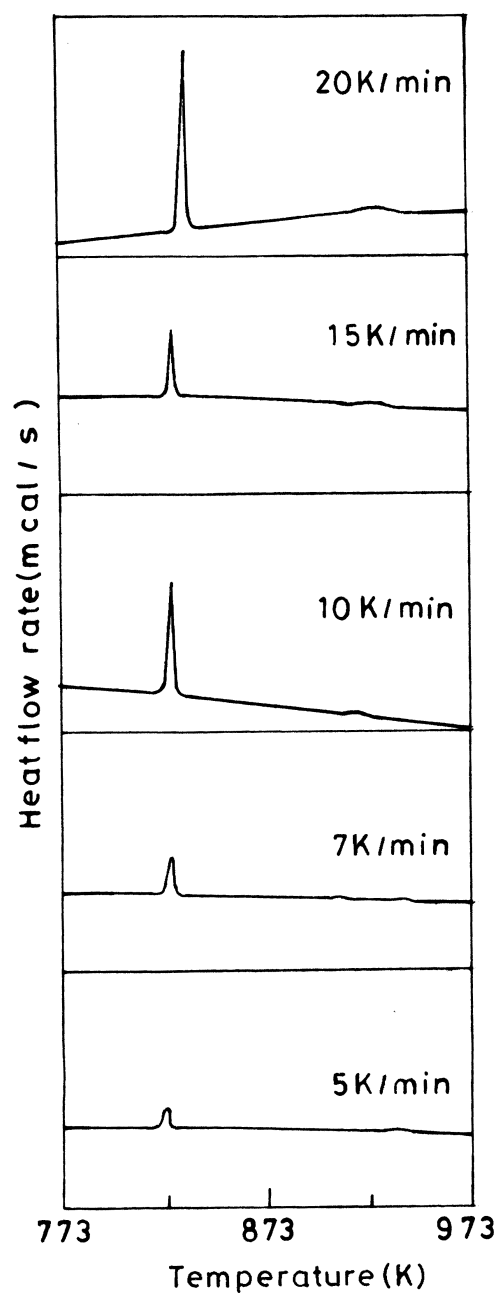**Figure 5.** DSC thermograms of irradiated Co–Ni glass at the heating rate of 5 K/min, 7 K/min, 10 K/min, 15 K/min and 20 K/min (fluence: 1×10^{13} ions/cm²).

Table 1. Variation of crystallization temperatures with heating rate and different nature of the $Co_{66}Si_{16}Fe_4B_{12}Mo_2$ glass.

Sample	Heating rate (K/min)	Crystallization temperature		Peak crystallization temperature	
		T_{c1} (K)	T_{c2} (K)	T_{p1} (K)	T_{p2} (K)
Virgin	5	819	877	829	908
	7	821	888	832	913
	10	825	894	837	920
	15	828	897	838	926
	20	830	898	841	928
Irradiated (fluence 1×10^{11} ions/cm^2)	5	819	877	828	908
	7	821	887	832	913
	10	825	894	837	919
	15	827	896	838	925
	20	830	897	841	928
Irradiated (fluence 1×10^{12} ions/cm^2)	5	819	877	828	908
	7	821	887	831	913
	10	825	894	837	920
	15	827	896	838	925
	20	830	898	841	928
Irradiated (fluence 1×10^{13} ions/cm^2)	5	819	877	828	908
	7	820	887	832	913
	10	825	894	837	920
	15	827	896	839	926
	20	830	898	841	928

Table 2. Variation of crystallization temperatures with heating rate and different nature of the $Co_{66}Si_{15}Fe_4B_{14}Ni_1$ glass.

Sample	Heating rate (K/min)	Crystallization temperature		Peak crystallization temperature	
		T_{c1} (K)	T_{c2} (K)	T_{p1} (K)	T_{p2} (K)
Virgin	5	820	897	823	918
	7	824	905	827	924
	10	828	908	831	931
	15	831	911	836	935
	20	836	918	839	937
Irradiated (fluence 1×10^{11} ions/cm^2)	5	820	897	823	918
	7	824	905	827	924
	10	828	907	831	932
	15	830	911	836	936
	20	836	917	839	938
Irradiated (fluence 1×10^{12} ions/cm^2)	5	820	897	823	918
	7	824	905	827	924
	10	828	907	831	931
	15	831	911	836	935
	20	835	918	839	937
Irradiated (fluence 1×10^{13} ions/cm^2)	5	820	896	823	918
	7	824	905	827	925
	10	828	908	831	931
	15	831	910	836	935
	20	836	918	839	938

The T_c and T_p values of both the glasses (irradiated alongwith virgin specimens) have been listed in tables 1 and 2. The above observation may be explained by the fact that the high-energy heavy ions passing through solids lose most of their energy through the electronic excitations (ionization) of target atom. The immediate consequences of electronic excitations are atomic rearrangements under certain conditions. Atomic displacements induced by electronic excitations were identified and established by Klaumunzer and Schumacher (1981) and Hou Ming-dou *et al* (1990) by observing radiation-induced growth in metallic glasses. However, no new phase has formed during high-energy heavy ion irradiation. It seems that whatever defects produced due to the irradiation are recovered at temperatures well below those necessary to induce crystallization during heat treatment given to the system.

Further, to gain more information about the kinetics of crystallization of irradiated samples in terms of kinetic parameters viz. activation energy, Avrami exponent and dimensionality of growth etc, the two theoretical models given by Kissinger (1956) and Gao and Wang (1986) have been used.

The Kissinger equation is given by

$$\ln(a/T_p^2) = -E_c/RT_p + \text{constant},$$

where a is the heating rate, T_p the peak crystallization temperature. The plot of $\ln(a/T_p^2)$ vs $1000/T_p$ yields a straight line and the slope of this straight line gives the activation energy, E_c.

Further, using the Gao and Wang model, the details of the kinetics of crystallization have been obtained through the determination of other parameters along with activation energy. The model gives a linear relationship between $\ln(dX/dt)_p$ and $1000/T_p$, and is given by

$$\ln(dX/dt)_p = -E_c/RT_p + \text{constant},$$

where, $(dX/dt)_p$ is the rate of transformed volume fraction at the peak of crystallization, T_p the peak crystallization temperature, E_c the activation energy and R the gas constant. E_c is determined from the slope of the straight-line plot of the above equation. As mentioned earlier, the two exothermic events at all the heating rates, in Co–Mo glass overlap each other to some extent. The first transformation is not fully completed before the second one begins.
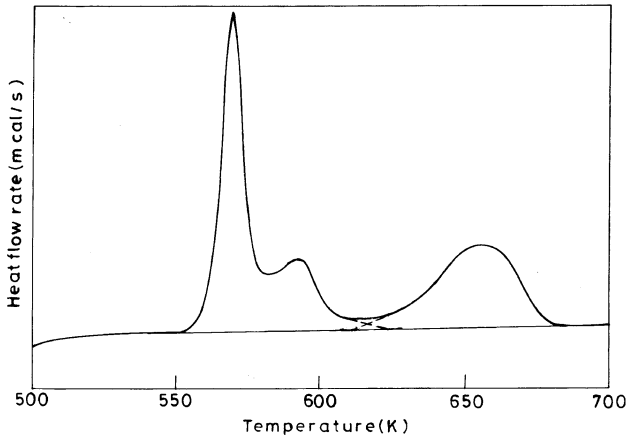

Figure 6. DSC trace of Co–Mo glass at the heating rate of 20 K/min as a representative curve for showing the partition of two overlapping peaks of crystallization by systematic extrapolation.
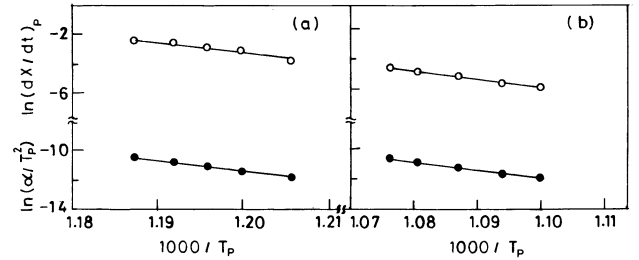

Figure 7. Kissinger's (●) and Gao-Wang (○) plots for irradiated Co–Mo glass (fluence: 1×10^{13} ions/cm^2): (**a**) for first crystallization and (**b**) second crystallization.

Table 3. Activation energy of crystallization of glasses.

| | Activation energy (kJ/mole) | | | | | |
| | Kissinger eq. | | Gao-Wang eq. | | Avrami exponent | |
Compositions	I peak	II peak	I peak	II peak	I peak	II peak
$Co_{66}Si_{16}Fe_4B_{12}Mo_2$						
a. Irradiated (fluence 1×10^{13} ions/cm^2)	632 ± 7	465 ± 7	627 ± 10	446 ± 10	2	1
b. Virgin sample	655 ± 7	459 ± 5	648 ± 10	459 ± 10	2	1
$Co_{66}Si_{15}Fe_4B_{14}Ni_1$						
a. Irradiated (fluence 1×10^{13} ions/cm^2)	508 ± 7	469 ± 7	493 ± 10	458 ± 10	9	2
b. Virgin samples	506 ± 7	472 ± 5	491 ± 10	460 ± 10	9	2

Further, the second phase has not begun to form at T_{p1}, peak crystallization temperature for the first transformation and similarly, the first transformation is completed prior to T_{p2}, peak crystallization temperature of the second transformation. Thus, the crystallization curve has been divided into two parts by systematic extrapolation of the two peaks for the calculation of rate of transformed volume fraction as shown in figure 6. The small peak (shoulder) due to delayed crystallization ($\leq 5\%$ of the main peak) is included in the main peak. In the case of Co–Ni glass no such problem occurs since the peaks are separated by wide temperature interval.

Kissinger and Gao-Wang plots of irradiated specimens are given in figures 7 and 8 for Co–Mo and Co–Ni glass, respectively. The activation energies computed from the slopes of straight lines are reported in table 3. The E_c values of both the virgin glasses (Jain *et al* 2000) are also given in the same table. It can be noted from the table that there is no remarkable difference in the activation energy for both stages of crystallization for irradiated and virgin samples. The observed difference in the E_c values is due to small changes in T_p values of virgin and irradiated samples. Even a difference of the order of 0·2–0·4 K (< 1 K) in T_p values brings an appreciable change in E_c values (of the order of ± 25 kJ/mole). Further, the activation energy for second crystallization in both the specimens is lower than that of first crystallization, which indicates an increase of driving force for second crystallization i.e. easier nucleation for the Co_3B b.c.t. phase. The difference in the values of activation energy computed through the two models may be attributed to basic assumptions lying in the two theories discussed elsewhere (Jain *et al* 2001).

In addition to activation energy, the variation of transformed volume fraction with temperature during both crystallization stages for both the glasses at the heating rate of 10 K/min has been shown in figures 9 and 10. It is evident from the figures that the percentage of transformed volume fraction during crystallization is exactly same for all the irradiated and virgin specimens. Thus, the above result ensures the same activation energy of all the specimens as the rate of crystallized volume fraction is same in virgin and irradiated specimens.
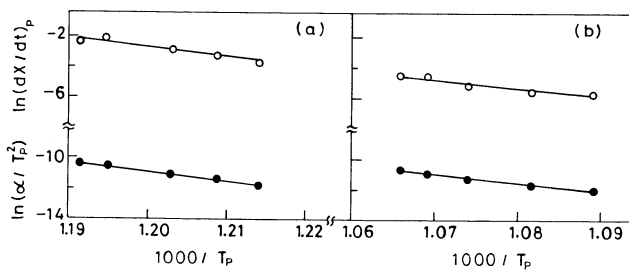
To obtain the information about morphology of growth and Avrami exponent, the following relations from Gao-Wang model have been used

$$K = K_0 \exp(- E_c/RT),$$

$$K_p = a\, E_c/RT_p^2,$$

$$(dX/dt)_p = 0.37\, nK_p,$$

where n is Avrami exponent, K_p the reaction rate factor, K_0 the frequency factor and other symbols have their usual meanings. In the case of Co–Mo glass, the average value of n comes out to be 2 and 1 for first and second crystallization stages, respectively. The n values for both the crystallization stages indicate one-dimensional growth along with surface crystallization. On the other hand, in Co–Ni glass, for first crystallization stage, the average value of n comes out to be ~ 9 while it decreases to 2 in case of second crystallization. The n value for first stage of crystallization indicates very high nucleation rate with three-dimensional growth while crystals grow in one dimension during the second crystallization. The values of n verify fast crystallization of first phase as compared to the second one; the temperature duration is very short in
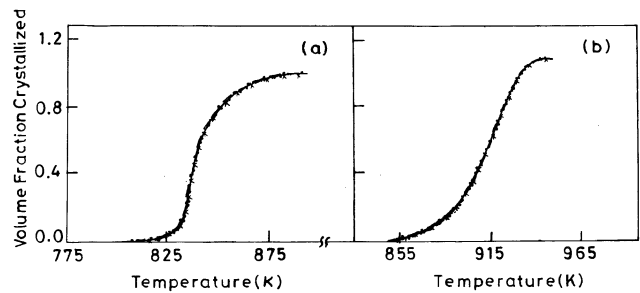

Figure 9. Volume fraction transformed as a function of temperature for Co–Mo glass at a heating rate of 10 K/min. (**a**) first crystallization and (**b**) second crystallization (— Virgin; –×–×–×– irradiated at fluence 1×10^{11} ions/cm^2; –•–•–•– irradiated at fluence 1×10^{12} ions/cm^2; • • • irradiated at fluence 1×10^{13} ions/cm^2).
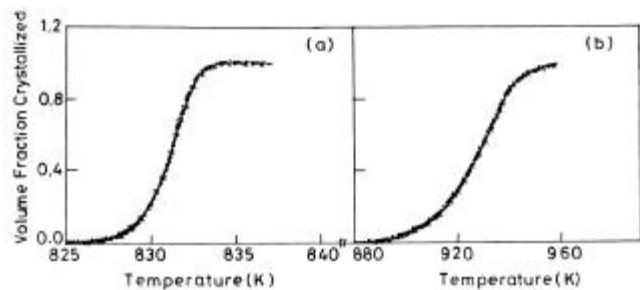

Figure 10. Volume fraction transformed as a function of temperature for Co–Ni glass at a heating rate of 10 K/min. (**a**) first crystallization and (**b**) second crystallization (— Virgin; –×–×–×– irradiated at fluence 1×10^{11} ions/cm^2; –•–•–•– irradiated at fluence 1×10^{12} ions/cm^2; • • • irradiated at fluence 1×10^{13} ions/cm^2).

Figure 8. Kissinger's (●) and Gao-Wang (o) plots for irradiated Co–Ni glass (fluence: 1×10^{13} ions/cm^2): (**a**) for first crystallization and (**b**) second crystallization.

the case of first crystallization as compared to the second one. The values of *n* for both glasses (irradiated and virgin) are listed in table 3. It is clear from the table that after irradiation, there is no change in the Avrami exponent, hence the morphology of growth does not change. The reason behind this may be again the recovery of defects during the heat treatment given to the system. The results of specimens irradiated at different fluences also agree with the results of present irradiated sample.

The above results suggest that irradiation of Ni^{11+} ions with the energy of 150 MeV at different fluences ranging from 10^{11} to 10^{13} ions/cm^2 do not affect the thermal stability against crystallization of Co-based metallic glasses in any way. The irradiation of further high energy (up to few GeV) may have some influence on the devitrification kinetics of these glasses. The attempts are going on in this direction.

4. Conclusions

The present study, dealing with effect of irradiation of fluences ranging from 10^{11} to 10^{13} ions/cm^2 on crystallization kinetics of Co-based glasses, reveals that, systems possibly with different atomic arrangements due to high-energy heavy ion irradiation, crystallize into same phase, even at same temperature. The high-energy heavy ion irradiation does not bring any discernible change in the crystallization kinetics. The defects due to irradiation are recovered well below the temperature necessary for crystallization during the thermal treatment given to the system. Both the glasses crystallize into two phases. The large value of Avrami exponent during first crystallization in Co–Ni glass shows a very high nucleation rate with three-dimensional growth.

References

Appleton B L, Sartwell B, Peercy P S, Schaefer R and Osgood R 1985 *Mater. Sci. & Engg.* **70** 23
Gao Y Q and Wang W 1986 *J. Non-Cryst. Solids* **87** 129
Graydon J W, Thorpe S J and Kirk D W 1995 *Acta Metall. Mater.* **43** 1363
Greer A L 1982 *Acta Metall.* **30** 171
Holzer J C and Kelton K F 1991 *Acta Metall. Mater.* **39** 1833
Hou Ming-dou, Klaumunzer S and Schmacher G 1990 *Phys. Rev.* **B41** 1144
Jain Rohit, Bhandari Deepika, Saxena N S and Sharma S K 2000 *J. Thermal Anal.* (communicated)
Jain Rohit, Saxena N S, Bhandari Deepika and Sharma S K 2001 *Mater. Sci. & Engg.* **A298** 51
Kissinger H E 1956 *J. Res. NBS* **57** 217
Klaumunzer S and Schumacher G 1981 *Phys. Rev. Lett.* **51** 1987
Köster U and Herold U 1981 *Glassy metals I* (ed.) H Beck and H J Guntherodt (Berlin: Springer-Verlag) p. 25 and references therein
Mehta G K 1994 *Phys. Education* **11** 245
Rauhala E, Ahlgren T, Vakevainen K, Raisanen J and Keinonen 1998 *J. Appl. Phys.* **83** 738
Wang Yuming and Chaofu Meng 1983 *J. Non-Cryst. Solids* **54** 187
Zhou Fie, He Kai-Yuan and Man Ling-Su 1994 *Mater. Sci. & Engg.* **A181/182** 1419